Check for updates

Polymerization-like kinetics of the self-assembly of colloidal nanoparticles into supracolloidal polymers†

Xiaodong Ma, Yaru Zhou, Liangshun Zhang, (iD) * Jiaping Lin (iD) * and Xiaohui Tian

The self-assembly of colloidal nanoparticles is conceptually analogous to the polymerization of reactive monomers in molecular systems. However, less is known about the polymerization of colloidal nanoparticles into supracolloidal polymers. Herein, using coarse-grained molecular dynamics and theoretical analysis, we reveal the self-assembly mechanism and kinetics of colloidal nanoparticles constructed from triblock terpolymers. The results show that the formation pathway of supracolloidal polymers involves monomer condensation and oligomer coalescence through the manner of end-to-end collisions. In contrast to the polymerization kinetics of molecular systems, the simulations and theoretical analysis definitely demonstrate that the growth of supracolloidal polymers obeys diffusion-controlled step-growth polymerization kinetics with a variable rate coefficient, where the growth rate is dependent upon the concentration of colloidal nanoparticles and the molecular information of triblock terpolymers. Our findings possess wide implications for understanding the growth of supracolloidal polymers, which is important for the rational and precise design of one-dimensional self-assembled superstructures with new horizons for biomedical applications.

Introduction

Synthetic supracolloidal polymers, formed through the one-dimensional self-assembly of colloidal nanoparticles, are captivating the minds of scientists due to their dynamic and responsive characteristics reminiscent of many living organisms, which make them extremely interesting for the fabrication of novel functional materials with promising applications in soft nanotechnology and biotechnology.[1–7] Recently, researchers have pursued a diversity of strategies to construct supracolloidal polymers *via* the self-assembly of soft materials such as peptide amphiphiles,[8,9] DNA,[10–12] amphiphilic block copolymers,[13–15] triblock terpolymers[16–19] and functionalized nanoparticles.[20–24] In these instances, Müller's group proposed a hierarchical self-assembly strategy to prepare well-defined supracolloidal polymers through utilizing triblock terpolymers of polystyrene-*block*-polybutadiene-*block*-poly(methylmethacrylate) (PS-*b*-PB-*b*-PMMA).[18,19] The patchy

colloidal nanoparticles initially originate from spherical micelles of triblock terpolymers and then self-assemble into supracolloidal polymers due to change of the solvent environment. In spite of these experimental advances, the mesoscopic details about self-assembly mechanisms and kinetics of colloidal nanoparticles have remained to be clearly elucidated.

Polymerization, the process of organization of small molecules into macromolecules, provides a conceptual framework to capture the formation of supracolloidal polymers due to their similarity in the self-repeating feature of building blocks. Extension of such a framework for molecular systems to the self-assembly of colloidal nanoparticles will be helpful to rationally design novel materials of supracolloidal polymers. However, due to the reduced size of colloidal nanoparticles, it is cumbersome to acquire the high-resolution details of polymerization-like kinetics at the mesoscopic scale.[25–28] A deep understanding of the polymerization-like kinetics for the self-assembly of colloidal nanoparticles (*e.g.*, how the colloidal nanoparticles self-assemble into the supracolloidal polymers and how the self-assembly kinetics is tuned by the physico-chemical properties of tailor-made nanoparticles) is one crucial theme to be resolved for their specific applications by virtue of biological responsiveness. From the point of view of experimental techniques used, it is prohibitively difficult and more challenging to witness the polymerization-like events

Shanghai Key Laboratory of Advanced Polymeric Materials, State Key Laboratory of Bioreactor Engineering, Key Laboratory for Ultrafine Materials of Ministry of Education, School of Materials Science and Engineering, East China University of Science and Technology, Shanghai 200237, China. E-mail: zhangls@ecust.edu.cn, jlin@ecust.edu.cn
†Electronic supplementary information (ESI) available: Model and additional simulation results. See DOI: 10.1039/c8nr05310c

occurring on a length scale of tens of nanometers and a time-scale of sub-milliseconds.

When experimental observations encounter difficulties, molecular simulations offer an alternative or complementary methodology to gain the detailed thermodynamic and kinetic information of complicated systems.[29–32] To comprehensively grasp the polymerization-like kinetics regarding the self-assembly of colloidal nanoparticles, we capitalize on a coarse-grained technique (i.e., dissipative particle dynamics abbreviated as DPD),[33–35] which is capable of resolving the events at the mesoscopic scale while maintaining a high-resolution description of nanostructures.

Herein, through combining large-scale molecular simulations and theoretical analysis, we present the first study of the polymerization-like kinetics regarding the self-assembly of colloidal nanoparticles, which are constructed from the triblock terpolymers via a stepwise self-assembly strategy. In contrast to the polymerization kinetics of molecular systems, our simulations clearly demonstrate that the diffusion behavior of colloidal nanoparticles plays a significant role in the formation of supracolloidal polymers via end-to-end collisions. Furthermore, the growth of supracolloidal polymers obeys step-growth polymerization kinetics with a variable rate coefficient, which can be tailored by the molecular information of triblock terpolymers. We also provide a theoretical analysis of the polymerization-like kinetics of colloidal nanoparticles, which is fully supported by simulation data.

Results and discussion

We utilize the DPD simulations to explore the polymerization-like assembly of colloidal nanoparticles constructed from the triblock terpolymers. The coarse-grained chains of polymers are mapped from PS-b-PB-b-PMMA terpolymers used by Müller's group.[18,19] Schematic representations of the mapping process are shown in Fig. 1a. For generality, the model chain of triblock terpolymers is denoted by the $A_xB_yC_z$ nomenclature, where the subscripts x, y and z respectively denote the lengths of A, B and C blocks. Full technical details of the simulation method and coarse-grained mapping are described in Part A of the ESI.†

To mimic the hierarchical self-assembly strategy in experiments, a stepwise self-assembly approach of triblock terpolymers in distinct solutions is proposed and conceptually illustrated in Fig. 1b. The miscibility between the I- and J-type components is described by the interaction parameter a_{IJ} (Table S3 of the ESI†). In the first-step assembly, the $A_xB_yC_z$ chains spontaneously aggregate into spherical micelles with dense B cores and mixed A/C coronas, because the A and C blocks exhibit good solubility in the S′ solvents (Part B of the ESI†). At the start of the second-step assembly, the S′ beads are replaced by the S beads, which are poor solvents for both A and B blocks. As a consequence, the spherical micelles evolve into aniso-tropic nanostructures with solvophobic A patches, whose valence (i.e., number of A patches) is controlled by the length
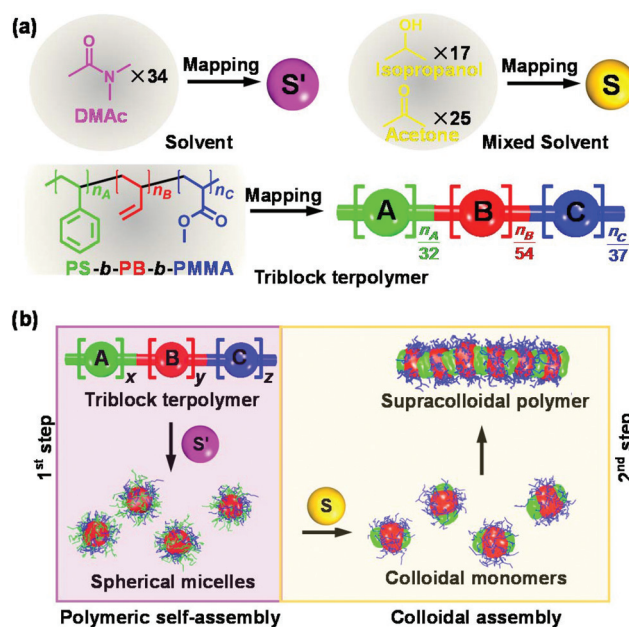

Fig. 1 (a) Schematic illustration of coarse-grained mapping for a realistic self-assembly system. The reference volume of one coarse-grained bead approximately equals the volume of 34 N,N-dimethylacetamide (DMAc) molecules (coded as S′ bead), mixed 17 isopropanol/25 acetone molecules (S bead), 32 styrene monomers (A bead), 54 butadiene monomers (B bead) or 37 methylmethacrylate monomers (C bead). (b) The stepwise self-assembly strategy of triblock terpolymers in dilute solution. 1st step: Triblock terpolymers dispersed in selective S′ solvents self-assemble into spherical micelles. 2nd step: Through modulation of solvent quality, colloidal nanoparticles from the spherical micelles self-assemble into supracolloidal polymers.

ratio x/y of solvophobic blocks of $A_xB_yC_z$ triblock terpolymers. Such intermediate nanostructures with distinct valences are regarded as colloidal nanoparticles. To further minimize the energy contribution from unfavorable A patch/solvent inter-faces, the colloidal nanoparticles undergo next-level assembly to yield spherical and linear superstructures (Part C of the ESI†). In particular, the linear superstructures are referred to as supracolloidal polymers.

In recent experiments, Müller's group reported a variety of multicompartment micelles with different internal components, which are regulated by the volume ratio of solvophobic blocks.[18,19] As shown in Fig. S4 and Table S4 of the ESI,† the polymer chains self-assemble into spherical and linear superstructures. More importantly, our simulations also demonstrate that these superstructures can be manipulated by the length ratio of solvophobic blocks (i.e., the molecular information of triblock terpolymers encodes effective parameters for regulating the high-level superstructures). Therefore, our DPD simulations reproduce the general characteristics of superstructures observed in the experiments, validating the coarse-grained model of the given experimental system. These encourage us to further explore the self-assembly mechanism and kinetics of colloidal nanoparticles, which are difficult to be evaluated in experiments.

Self-assembly mechanism of colloidal nanoparticles

Next, we focus on the formation process of superstructures from the pre-assembled divalent colloidal nanoparticles (also termed colloidal monomers). For simplicity, all the DPD simulations start from a random dispersion of M_0 monodisperse colloidal nanoparticles in the S solvents. The initial concentration of nanoparticles is denoted by $C_0 \equiv M_0/(N_A L^3)$, where L is the edge size of the simulation box and N_A is the Avogadro constant. The number of triblock terpolymer chains per nanoparticle has a value of 60, corresponding to the peak position of the probability distribution of chain number in spherical micelles (Fig. S2d–S2f of the ESI†). As shown in Part D of the ESI,† the divalent colloidal monomers condense with neighboring nanoparticles and self-assemble into colloidal oligomers (termed condensation events of colloidal monomers). Coalescence events of colloidal oligomers also take place and longer supracolloidal polymers are finally formed.

To gain detailed insight into the self-assembly behaviors of colloidal nanoparticles, we monitor the motions of superstructures in the DPD simulations. As a representative example, Fig. 2a shows the temporal evolution of center dis-

tance d between a pair of colloidal nanoparticles and the corresponding configurations of the nanoparticle pair. Initially, two colloidal nanoparticles are separated by a long distance. The Brownian motions of colloidal nanoparticles induce random collisions with each other. When collisions of colloidal nanoparticles occur at the solvophilic C coronas (e.g., manners of side-to-side (abbreviated as SS) and side-to-end (SE) collisions), the lateral repulsions of C blocks push away the colloidal nanoparticles and prevent subsequent contacts between distinct A patches. Such an elastic event is quantitatively reflected by the trajectory of colloidal nanoparticles in the range of time $0 < t < 110.0$ μs. In contrast, end-to-end (EE) collisions of colloidal nanoparticles are able to circumvent the obstacles of solvophilic C blocks and lead to effective collisions. Once the end-to-end collisions take place, such a particular orientation to bind the solvophobic A patches triggers the 'reaction' of colloidal nanoparticles, and the colloidal superstructures are quickly formed. As shown in Fig. 2a, such a 'reaction' of solvophobic A patches is also confirmed by a sharp decrease of center distance d in ~10.0 μs, in comparison with the long diffusion time of colloidal nanoparticles. It should be stressed that the formed physical bonds connecting two separated B domains are permanent and cannot be broken.

A number of quantities are examined to characterize the dominant roles in the colloidal self-assembly. One relevant quantity is the percentage of diffusion time in the self-assembly event of superstructures defined as $f_D = t_D/(t_D + t_R) \times 100\%$, where the diffusion time t_D and the 'reaction' time t_R are highlighted in Fig. 2a. Another quantity characterizing the effective collisions is provided by the percentage of end-to-end collisions defined as $f_{EE} = n_{EE}/(n_{SS} + n_{SE} + n_{EE}) \times 100\%$, where n_{SS}, n_{SE} and n_{EE} respectively denote the numbers of side-to-side, side-to-end and end-to-end collisions occurring in each time interval. As shown in Fig. 2b, the diffusion time accounts for more than 90%, suggesting that the diffusion stage plays a significant role in controlling the formation of supracolloidal polymers. As shown in Fig. 2c, the percentage of end-to-end collisions is less than 1.0%, because the translation and rotation of whole superstructures to an appropriate alignment are required to realize the effective collisions. Once the end-to-end collisions take place, physical bonds are formed.

Fig. 2d summarizes all the self-assembly pathways of colloidal nanoparticles that we can observe in the formation of supracolloidal polymers. The formation pathways of supracolloidal polymers involve two distinct processes: condensation of colloidal monomers and coalescence of colloidal oligomers. In each process, the directional aggregation of colloidal nanoparticles leads to complex mechanisms of dynamical conversion between various superstructures. In general, two distinctive characteristics are derived from the mechanisms: the first is that the process of colloidal self-assembly includes the diffusion and 'reaction' stages, but the diffusion of superstructures plays a dominant role in the growth of supracolloidal polymers (i.e., diffusion-controlled cluster–cluster aggregation);[36] and the second is that only end-to-end collisions effec-
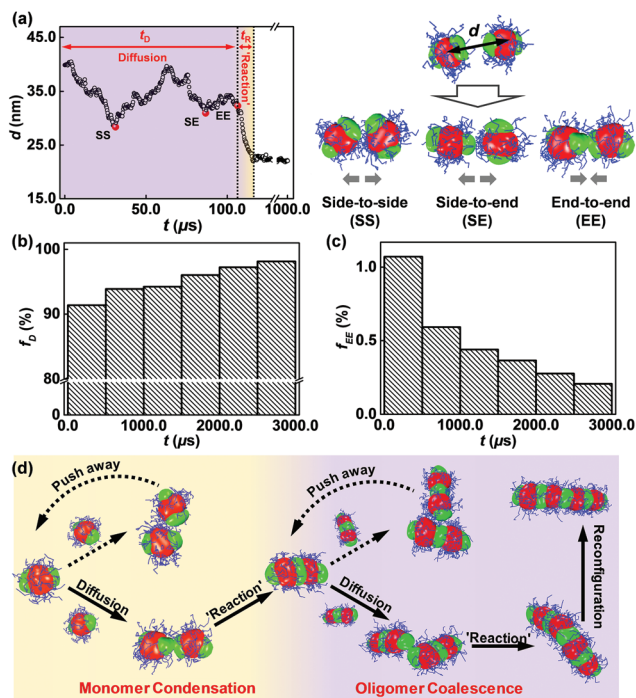

Fig. 2 (a) Temporal evolution of center distance d between a pair of colloidal nanoparticles in a typical self-assembly event. The self-assembly process of colloidal nanoparticles is divided into diffusion and 'reaction' stages. The right panel shows side-to-side (abbreviated as SS), side-to-end (SE) and end-to-end (EE) collisions of nanoparticle pairs. (b) Percentage f_D of diffusion time in the course of self-assembly of colloidal nanoparticles. The diffusion time t_D and 'reaction' time t_R are highlighted in panel (a). (c) Percentage f_{EE} of effective collisions with respect to time t. The data are collected from a time interval of 500.0 μs. (d) Self-assembly pathways of colloidal nanoparticles observed in the formation of supracolloidal polymers. The background colors are used to distinguish processes of monomer condensation and oligomer coalescence.

tively generate the physical bonds connecting the super-structures (solid lines in Fig. 2d), whereas other collisions push away the colloidal superstructures due to the lateral repulsions of solvophilic C blocks (dashed lines). It is worthwhile mentioning that the soft and dynamic features of self-assembled superstructures promote reconfiguration to achieve the linear supracolloidal polymers in the process of oligomer coalescence. Therefore, the results from the DPD simulations provide new insight into the self-assembly of colloidal nanoparticles at the mesoscopic level (*i.e.*, the self-assembly of colloidal nanoparticles is the diffusion-controlled process *via* the manner of end-to-end collisions).

Self-assembly kinetics of colloidal nanoparticles

As illustrated above, the divalent colloidal nanoparticles behave as bifunctional molecules. In the supracolloidal polymers, the colloidal nanoparticles correspond to the repeating unit of molecular polymers and the non-terminal A patches act as the non-covalent (physical) bonds. The growth of such superstructures goes through the colloidal monomer → oligomer → polymer pathway, which is similar to the step-growth polymerization in molecular systems. We extend the polymerization kinetics of molecules to conceptualize the growth of supracolloidal polymers and predict the organization of colloidal nanoparticles. For the kinetic analysis, we keep track of the average number $\langle N \rangle_n$ of colloidal monomers in the supracolloidal polymers, concentration C_m of free colloidal nanoparticles, concentration C_p of supracolloidal polymers and polydispersity index (PDI) of supracolloidal polymers.

Fig. 3a plots the square $\langle N \rangle_n^2$ of the average number of colloidal monomers as a function of the time t. The variation in $\langle N \rangle_n^2$ follows a linear relationship in terms of the time. Fig. 3b and c depict the temporal dependence of the concentration C_m of free colloidal nanoparticles and the concentration C_p of supracolloidal polymers, respectively. The early stage of colloidal self-assembly is characterized by a rapid reduction of colloidal nanoparticles. During this stage, the superstructures mainly grow through the condensation of colloidal monomers into the colloidal dimers and trimers, and the concentration of supracolloidal polymers is increased. As time goes by, the colloidal nanoparticles are gradually depleted and the concentration of supracolloidal polymers reaches a maximum value. In the subsequent colloidal self-assembly, the dominant growth process of supracolloidal polymers shifts from the monomer condensation to the oligomer coalescence (highlighted by colors in Fig. 3c), which gives rise to consumption of colloidal oligomers. Fig. 3d shows the temporal dependence of the polydispersity index (PDI) of supracolloidal polymers. The PDI of growing supracolloidal polymers increases with time, and approaches the value of 2.

To provide a definitive confirmation of the step-growth polymerization (SGP) process for the self-assembly of colloidal nanoparticles, we propose a theoretical model to predict the growth of supracolloidal polymers. Considering the diffusion-controlled mechanism for the self-assembly of colloidal nanoparticles, our model follows the main idea of Leite and co-
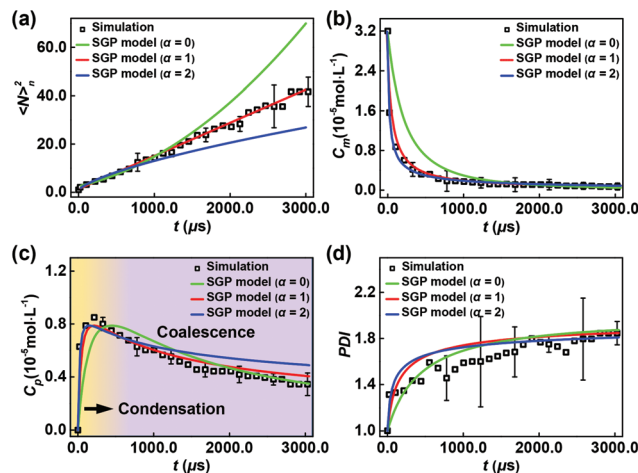

Fig. 3 Polymerization-like kinetics in the course of colloidal self-assembly. (a) Square $\langle N \rangle_n^2$ of the average number of colloidal monomers in supracolloidal polymers, (b) concentration C_m of free colloidal nanoparticles, (c) concentration C_p of supracolloidal polymers and (d) polydispersity index (PDI) of supracolloidal polymers as a function of the time t. The solid lines represent the fitted curves on the basis of the step-growth polymerization (SGP) model with various exponential factors α. The background colors in panel (c) are used to distinguish processes of monomer condensation and oligomer coalescence.

authors,[37] which is extension of the classic Flory model for the step-growth polymerization kinetics in molecular systems.[38,39] Consumption of building units (including colloidal nanoparticles and supracolloidal polymers with terminal A patches) obeys the following rate equation:

$$\frac{dC}{dt} = -kC^2 \tag{1}$$

where C is the concentration of building units. Unlike Flory's classic model where the rate coefficient k is assumed to be constant during the overall polymerization process, our modified model considers the fact that the mobility of building units is dependent upon their size. Namely, the variation of rate coefficient k can be estimated by the average number $\langle N \rangle_n$ of colloidal monomers in the supracolloidal polymers and the exponential factor α (*i.e.*, $k = k_0/\langle N \rangle_n^{\alpha}$),[40–42] where k_0 is the rate constant and $\langle N \rangle_n$ equals C_0/C (C_0 is the initial concentration of colloidal nanoparticles). As a special case, the exponential factor $\alpha = 0$ refers to the classic Flory model. Substituting these variables into eqn (1) yields the analytic expressions of relevant variables for the SGP model,

$$\langle N(t) \rangle_n^{\alpha+1} = K_1 t + 1 \tag{2}$$

$$C_m(t) = \frac{C_0}{[K_1 t + 1]^{\frac{2}{\alpha+1}}} \tag{3}$$

$$C_p(t) = \frac{C_0 \left[(K_1 t + 1)^{\frac{1}{\alpha+1}} - 1 \right]}{(K_1 t + 1)^{\frac{2}{\alpha+1}}} \tag{4}$$

$$\mathrm{PDI}(t) = 2 - \frac{1}{[K_1 t + 1]^{\frac{1}{\alpha+1}}} \quad (5)$$

where $K_1 = (\alpha + 1)k_0 C_0$ is the growth rate of supracolloidal polymers. Full technical details of the SGP model can be found in Part E of the ESI.†

In Fig. 3, the lines show the fitted curves to the simulation data based on eqn (2)–(5) with various exponential factors α. As shown in Fig. 3a, the classic SGP model with a constant rate coefficient (corresponding to the $\alpha = 0$ case) overpredicts the square $\langle N \rangle_n^2$ of the average number of colloidal monomers in the later stage of colloidal self-assembly. The modified model with $\alpha = 1$ well describes the growth of supracolloidal polymers. For the case of $\alpha = 2$, the modified model underestimates the values of $\langle N \rangle_n^2$. To evaluate the generality of the modified model, the temporal evolutions of C_m, C_p and PDI predicted by eqn (3)–(5) are also presented in Fig. 3b–d, respectively. Similar observations are also identified for the cases of C_m, C_p and PDI. Thus, the theoretical curves of the SGP model with $\alpha = 1$ well fit the simulation data, suggesting that the growth of supracolloidal polymers at the mesoscopic level obeys the step-growth polymerization kinetics with variable rate coefficient.

Similar to the polymerization kinetics in molecular systems, the growth rate K_1 of supracolloidal polymers in eqn (2)–(5) has a tight relation with the initial concentration C_0 of colloidal nanoparticles. Because the molecular information of tailor-made polymers is incorporated into the colloidal nanoparticles, physiochemical properties of triblock terpolymers would also impact the growth of supracolloidal polymers. Below, we probe into the effects of parameter settings of DPD simulations on the self-assembly kinetics of colloidal nanoparticles, including initial concentration of colloidal nanoparticles, compositions and interaction parameters of triblock terpolymers.

Fig. 4a shows the temporal evolution of the square $\langle N \rangle_n^2$ of the average number of colloidal monomers for various initial concentrations C_0 of colloidal nanoparticles. In the range of 1.2×10^{-5} mol L^{-1} $\leq C_0 \leq 3.2 \times 10^{-5}$ mol L^{-1}, the growth of supracolloidal polymers emerges in a similar way: the values of $\langle N \rangle_n^2$ are linearly proportional to the time t. A fit of simulation data to the linear relationship in eqn (2) (case of $\alpha = 1$) deduces the growth rate of supracolloidal polymers $K_1 = 0.0037$ μs^{-1}, 0.0087 μs^{-1} and 0.0135 μs^{-1} for $C_0 = 1.2 \times 10^{-5}$ mol L^{-1}, 2.4×10^{-5} mol L^{-1} and 3.2×10^{-5} mol L^{-1}, respectively. The inset of Fig. 4a shows the change of growth rate K_1 of supracolloidal polymers in terms of the initial concentration C_0 of colloidal nanoparticles. An increase of the concentration of colloidal nanoparticles accelerates their polymerization-like kinetics, because the diffusion time of building units becomes short. It is worthwhile pointing out that the dashed line in the inset of Fig. 4a represents the fitted curve of the growth rate K_1 of supracolloidal polymers in terms of the initial concentration C_0 of colloidal nanoparticles according to the relationship $K_1 = (\alpha + 1)k_0 C_0$, which yields a rate constant $k_0 = 1.9 \times 10^8$ L mol^{-1} s^{-1} for the colloidal self-assembly. It should be mentioned that
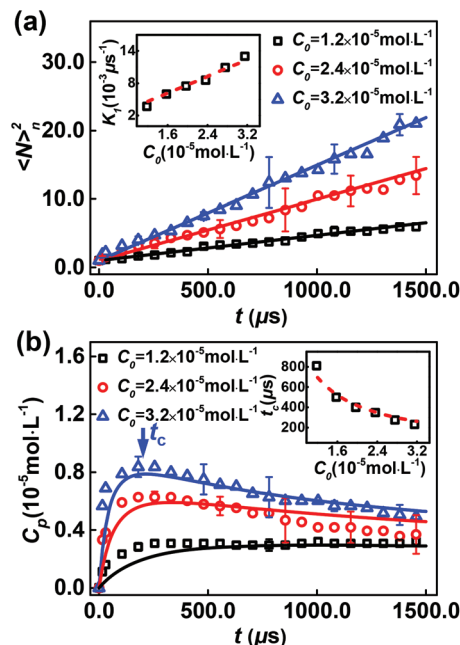

Fig. 4 Polymerization-like kinetics at various initial concentrations C_0 of colloidal nanoparticles. (a) Variation in the square $\langle N \rangle_n^2$ of the average number of colloidal monomers as a function of the time t at $C_0 = 1.2 \times 10^{-5}$ mol L^{-1}, 2.4×10^{-5} mol L^{-1} and 3.2×10^{-5} mol L^{-1}. The inset depicts the dependence of the growth rate K_1 of supracolloidal polymers on the initial concentration C_0 of colloidal nanoparticles, and the dashed line shows the relationship $K_1 \propto C_0$. (b) Variation in the concentration C_p of supracolloidal polymers with time t. The arrow highlights the characteristic time t_c, where C_p approaches the maximum value. The inset represents the characteristic time t_c as a function of the initial concentration C_0 of colloidal nanoparticles.

the initial concentration of micelles in the experiments is 1–2 orders of magnitude smaller than the values considered in the simulations.[18,19] As a consequence, the growth rate K_1 of supracolloidal polymers is much larger than that of experimental systems. However, the rate constant k_0 may be comparable to the experimental value, since the rate constant k_0 is independent of the initial concentration of colloidal nanoparticles.

Fig. 4b shows the effect of the initial concentration C_0 of colloidal nanoparticles on the concentration C_p of supracolloidal polymers. As the concentration of colloidal nanoparticles is increased, more supracolloidal polymers are formed. In addition, the availability of colloidal nanoparticles plays an important role in the growth process of supracolloidal polymers. Here, we introduce characteristic time t_c (highlighted by an arrow in Fig. 4b) to distinguish the growth pathway of supracolloidal polymers (i.e., condensation of colloidal monomers and coalescence of colloidal oligomers). As shown in the inset of Fig. 4b, the characteristic time t_c decreases with the initial concentration C_0 of colloidal nanoparticles. From the condition $dC_p/dt = 0$ at $t = t_c$ in eqn (4), one can obtain the relationship between the characteristic time and the initial concentration of colloidal nanoparticles, i.e., $t_c = 3/K_1$ or

equivalently $t_c = 3/(2k_0C_0)$. The dashed line in the inset of Fig. 4b shows the theoretically predicted values of t_c. The good agreement between the simulation data and the predicted values further supports the fact that the growth of supracolloidal polymers obeys step-growth polymerization kinetics with a variable rate coefficient.

Fig. 5 shows the growth rate K_1 of supracolloidal polymers in terms of the physiochemical properties of solvophilic C blocks. The polymerization-like kinetics in the system of colloidal nanoparticles obeys the $\langle N \rangle_n^2 \propto t$ relationship, which is depicted in Part F of the ESI.† The larger interaction parameter a_{CS} results in a noticeable acceleration of colloidal self-assembly (Fig. 5a). However, the long C blocks slow down the growth rate of supracolloidal polymers (Fig. 5b).

The exposed area S_A is introduced to clarify the effects of the physiochemical properties of triblock terpolymers on the polymerization-like kinetics. As schematically illustrated in the inset of Fig. 5a, S_A is defined as the exposed areas of terminal A patches, which are not shielded by the solvophilic C blocks and directly interact with the selective S solvents. When the solvophilicity of C blocks becomes weak (corresponding to an increase of a_{CS}), the tails of the C blocks are retracted from the A patches to relieve the contacts with selective S solvents. As a result, the exposed areas of solvophobic A patches are increased (Fig. 5a), implying that the probability of effective collisions of building units via the end-to-end manner is boosted. Thus, an increase of the interaction parameter a_{CS}

accelerates the polymerization-like kinetics. However, because the solvophilic C blocks are in the stretched configuration, the longer C blocks provide more space to shield the solvophobic A patches, corresponding to a decrease of the exposed area S_A (Fig. 5b) or probability of effective collisions of building units. Consequently, as the solvophilic C blocks become long, the colloidal nanoparticles slowly self-assemble into supracolloidal polymers.

It should be mentioned that the physiochemical properties of solvophobic A and B blocks also affect the polymerization-like kinetics of colloidal nanoparticles, which are illustrated in Part G of the ESI.† It is further demonstrated that the growth rate of supracolloidal polymers is dependent upon the exposed area of terminal A patches, which is tailored by the molecular information of triblock terpolymers such as block length and interaction parameter.

Discussion

Our findings from the DPD simulations demonstrate that the self-assembly of colloidal nanoparticles into supracolloidal polymers resembles many aspects of molecular step-growth polymerization, such as the manner of end-to-end collisions, linear shape of polymers and Flory's equation. Despite the physical analogies to molecular step-growth polymerization, there also exist some unique characteristics in the course of colloidal self-assembly. Specifically, the growth process of supracolloidal polymers is mainly determined by the diffusion stage instead of the 'reaction' stage (Fig. 2). Furthermore, the rate constant $k_0 \sim 10^8$ L mol^{-1} s^{-1} of colloidal self-assembly (derived from Fig. 4a) is remarkably larger than that of molecular step-growth polymerization (typically in the range of $\sim 10^{-3}$–10^{-5} L mol^{-1} s^{-1}).[39] In addition, the growth rate of supracolloidal polymers could be regulated by the exposed area of solvophobic patches instead of the activation energy of molecules, which provides new opportunity for fabricating one-dimensional self-assembled superstructures.

It should be mentioned that nanoparticles functionalized with homopolymers have emerged as a versatile strategy for constructing nanoparticle chains.[43–45] As a typical example, Kumacheva and co-workers demonstrated that the polymerization degree of nanoparticle chains could be predicted by step-growth polymerization kinetics in molecular systems, and estimated the rate constant of polymerization-like kinetics as $k_0 \sim 2.9 \times 10^4$ L mol^{-1} s^{-1}.[20] This rate constant is 4 orders of magnitude smaller than that of our system ($k_0 \sim 10^8$ L mol^{-1} s^{-1}), because the driving force of colloidal self-assembly from the solvophobic patches is much stronger. It is worthwhile mentioning that the rate constant derived from our simulations is comparable to the reported value ($\sim 10^7$ L mol^{-1} s^{-1}) for the polymerization-like kinetics of nanoplates.[27]

In comparison with the case of nanoparticles functionalized with homopolymers, another salient feature of our work is that the self-assembly kinetics of colloidal nanoparticles follows step-growth polymerization with a variable rate coeffi-
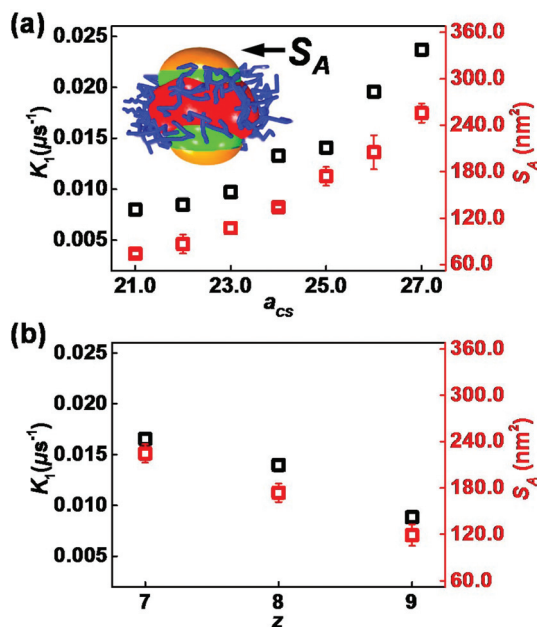

Fig. 5 Effects of the physiochemical properties of solvophilic C blocks on the polymerization-like kinetics. (a) Growth rate K_1 of supracolloidal polymers and exposed area S_A of terminal A patches as a function of the interaction parameter a_{CS}. The inset schematically illustrates the determination of exposed areas colored by yellow. (b) Growth rate K_1 of supracolloidal polymers and exposed area S_A of terminal A patches as a function of the length z of solvophobic C blocks.

cient (Fig. 3). However, the assembly of homopolymer-functio-
nalized nanoparticles matches step-growth polymerization
with a constant coefficient.[20] The differences stem from the
flexibility of self-assembled superstructures, implying that the
end-to-end collisions of homopolymer-functionalized nano-
particles do not require the motion of whole super-structures
(Part H of the ESI†).[38,39] These differences highlight the impor-
tance of structures and properties of nanoscale building units
in determining their self-assembly mechanism and kinetics,
which provide useful guidelines for experimentalists to
construct polymer-like superstructures with predictable size
and shape.

In the present work, monodisperse colloidal nanoparticles
with the chain number $n_{chain} = 60$ of triblock terpolymers are
chosen as the initial configuration of simulations at the
second-step assembly. We also simulate the formation of
superstructures under the conditions of various initial
configurations and annealing processes. As shown in Parts I
and J of the ESI,† the growth of superstructures generally
obeys step-growth polymerization kinetics.

Conclusions

In conclusion, the formation of supracolloidal polymers
involves monomer condensation and oligomer coalescence *via*
end-to-end collisions. More importantly, it is clearly demon-
strated that the growth of supracolloidal polymers obeys
diffusion-controlled step-growth polymerization kinetics with
a variable rate coefficient, which has not been definitely veri-
fied in experiments so far. Furthermore, their growth rate is
strongly dependent upon the initial concentration of colloidal
nanoparticles and the exposed area of solvophobic patches,
which can be finely tuned by molecular information of triblock
terpolymers. Our simulations provide a unique picture of the
roles of the stepwise self-assembly strategy as well as mono-
disperse colloidal nanoparticles for achieving the rational and
precise design of supracolloidal polymers.

Conflicts of interest

There are no conflicts to declare.

Acknowledgements

Notes and references

1 G. M. Whitesides and B. Grzybowski, *Science*, 2002, **295**, 2418–2421.

2 A. Walther and A. H. E. Müller, *Chem. Rev.*, 2013, **113**, 5194–5261.

3 L. Zhang and S. C. Glotzer, *Nano Lett.*, 2004, **4**, 1407–1413.

4 S. C. Glotzer and M. Solomon, *Nat. Mater.*, 2007, **6**, 557–562.

5 A. H. Gröschel and A. H. E. Müller, *Nanoscale*, 2015, **7**, 11841–11876.

6 L. J. Hill, N. Pinna, K. Char and J. Pyun, *Prog. Polym. Sci.*, 2015, **40**, 85–120.

7 M. R. Jones, K. D. Osberg, R. J. MacFarlane, M. R. Langille and C. A. Mirkin, *Chem. Rev.*, 2011, **111**, 3736–3827.

8 Z. Zhuang, T. Jiang, J. Lin, L. Gao, C. Yang, L. Wang and C. Cai, *Angew. Chem., Int. Ed.*, 2016, **55**, 12522–12527.

9 C. Yang, L. Gao, J. Lin, L. Wang, C. Cai, Y. Wei and Z. Li, *Angew. Chem., Int. Ed.*, 2017, **56**, 5546–5550.

10 T. Tigges, T. Heuser, R. Tiwari and A. Walther, *Nano Lett.*, 2016, **16**, 7870–7874.

11 Q. Yu, X. Zhang, Y. Hu, Z. Zhang and R. Wang, *ACS Nano*, 2016, **10**, 7485–7492.

12 W. B. Rogers, W. M. Shih and V. N. Manoharan, *Nat. Rev. Mater.*, 2016, **1**, 16008.

13 T. Gädt, N. S. Ieong, G. Cambridge, M. A. Winnik and I. Manners, *Nat. Mater.*, 2009, **8**, 144–150.

14 J.-H. Kim, W. J. Kwon and B.-H. Sohn, *Chem. Commun.*, 2015, **51**, 3324–3327.

15 S. Lee, S. Jang, K. Kim, J. Jeon, S. S. Kim and B. H. Sohn, *Chem. Commun.*, 2016, **52**, 9430–9433.

16 Z. Li, E. Kesselman, Y. Talmon, M. A. Hillmyer and T. P. Lodge, *Science*, 2004, **306**, 98–101.

17 H. Cui, Z. Chen, S. Zhong, K. L. Wooley and D. J. Pochan, *Science*, 2007, **317**, 647–650.

18 A. H. Gröschel, F. H. Schacher, H. Schmalz, O. V. Borisov, E. B. Zhulina, A. Walther and A. H. E. Müller, *Nat. Commun.*, 2012, **3**, 710.

19 A. H. Gröschel, A. Walther, T. I. Löbling, F. H. Schacher, H. Schmalz and A. H. E. Müller, *Nature*, 2013, **503**, 247–251.

20 K. Liu, Z. Nie, N. Zhao, W. Li, M. Rubinstein and E. Kumacheva, *Science*, 2010, **329**, 197–200.

21 Q. Chen, J. K. Whitmer, S. Jiang, S. C. Bae, E. Luijten and S. Granick, *Science*, 2011, **331**, 199–202.

22 Y. Wang, Y. Wang, D. R. Breed, V. N. Manoharan, L. Feng, A. D. Hollingsworth, M. Weck and D. J. Pine, *Nature*, 2012, **491**, 51–55.

23 K. Liu, N. Zhao and E. Kumacheva, *Chem. Soc. Rev.*, 2011, **40**, 656–671.

24 X. Zhang, L. Lv, G. Wu, D. Yang and A. Dong, *Chem. Sci.*, 2018, **9**, 3986–3991.

25 L. Albertazzi, D. van der Zwaag, C. M. A. Leenders, R. Fitzner, R. W. van der Hofstad and E. W. Meijer, *Science*, 2014, **344**, 491–495.

26 B. Luo, J. W. Smith, Z. Ou and Q. Chen, *Acc. Chem. Res.*, 2017, **50**, 1125–1133.

27 B. Luo, J. W. Smith, Z. Wu, J. Kim, Z. Ou and Q. Chen, *ACS Nano*, 2017, **11**, 7626–7633.

28 J. Kim, Z. Ou, M. R. Jones, X. Song and Q. Chen, *Nat. Commun.*, 2017, **8**, 761.

29 S. Jiang, J. Yan, J. K. Whitmer, S. M. Anthony, E. Luijten and S. Granick, *Phys. Rev. Lett.*, 2014, **112**, 218301.

30 R. Guo, J. Mao, X.-M. Xie and L.-T. Yan, *Sci. Rep.*, 2014, **4**, 7021.

31 L. Ruiz and S. Keten, *J. Phys. Chem. Lett.*, 2014, **5**, 2021–2026.

32 S. M. Bromfield, P. Posocco, C. W. Chan, M. Calderon, S. Guimond, J. E. Turnbull, S. Pricl and D. K. Smith, *Chem. Sci.*, 2014, **5**, 1484–1492.

33 P. J. Hoogerbrugge and J. M. V. A. Koelman, *Europhys. Lett.*, 1992, **19**, 155–160.

34 P. Espanõl and P. Warren, *Europhys. Lett.*, 1995, **30**, 191–196.

35 R. D. Groot and P. B. Warren, *J. Chem. Phys.*, 1997, **107**, 4423–4435.

36 M. Y. Lin, H. M. Lindsay, D. A. Weitz, R. Klein, R. C. Ball and P. Meakin, *J. Phys.: Condens. Matter*, 1990, **2**, 3093–3113.

37 C. Ribeiro, E. J. H. Lee, E. Longo and E. R. Leite, *ChemPhysChem*, 2006, **7**, 664–670.

38 P. J. Flory, *Principles of Polymer Chemistry*, Cornell University Press, Ithaca, 1953.

39 G. Odian, *Principles of Polymerization*, John Wiley & Sons, Inc., Hoboken, 4th edn, 2004.

40 M. Doi, *Chem. Phys.*, 1975, **9**, 455–466.

41 M. Doi, *Chem. Phys.*, 1975, **11**, 115–121.

42 J. D. Guzmán, R. Pollard and J. D. Schieber, *Macromolecules*, 2005, **38**, 188–195.

43 G. A. DeVries, M. Brunnbauer, Y. Hu, A. M. Jackson, B. Long, B. T. Neltner, O. Uzun, B. H. Wunsch and F. Stellacci, *Science*, 2007, **315**, 358–361.

44 T. Mirkovic, M. L. Foo, A. C. Arsenault, S. Fournier-Bidoz, N. S. Zacharia and G. A. Ozin, *Nat. Nanotechnol.*, 2007, **2**, 565–569.

45 Z. Nie, D. Fava, E. Kumacheva, S. Zou, G. C. Walker and M. Rubinstein, *Nat. Mater.*, 2007, **6**, 609–614.